Organometallics **2000,** *19,* 1983−1992

Studies with the Ruthenacarborane Complex [Ru(CO)(PPh_3)(THF)(η^5-7,8-$C_2B_9H_{11}$)]: Reactions with Terminal Alkynes[†]

Shaowu Du, Dianne D. Ellis, Paul A. Jelliss, Jason A. Kautz,
John M. Malget, and F. Gordon A. Stone*

Department of Chemistry and Biochemistry, Baylor University, Waco, Texas 76798-7348

Received January 10, 2000

The syntheses of the complexes [Y][RuX(L)(PPh_3)(η^5-7,8-$C_2B_9H_{11}$)] (X = Cl, Y = K(18-crown-6), L = CO (**1**), PPh_3 (**2**); X = I, Y = NEt_4, L = CO (**3**)) are reported, and the structure of **3** has been established by an X-ray diffraction study. The anion adopts the “piano stool” structure with the ruthenium atom η^5-coordinated on one side by a *nido*-7,8-$C_2B_9H_{11}$ group and on the other by the CO, PPh_3, and I ligands. Treatment of **1** with $TlPF_6$ in THF (tetrahydrofuran) affords solutions of the labile species [Ru(THF)(CO)(PPh_3)(η^5-7,8-$C_2B_9H_{11}$)] (**5**), which readily react with a 3-fold excess of the monosubstituted alkynes RC≡CH (R = Ph, Bu^t, $SiMe_3$). The product from PhC≡CH is [Ru(CO)(PPh_3)(η^2: η^5-9-(*E*)-C(H)=C(H)Ph-7,8-$C_2B_9H_{10}$)] (**8**), the structure of which was determined by X-ray crystallography. The metal atom is η^5-coordinated by the open face of the *nido*-7,8-C_2B_9 cage and also η^2-coordinated by the C=C bond of the *E*-C(H)=C(H)Ph group, the latter being attached to a boron atom in an α-site with respect to the carbons of the $\overline{\text{CCBBB}}$ ring ligating the ruthenium. Reaction between **5** and Bu^{t}C≡CH gives [Ru(CO)(PPh_3)(η^2: η^5-9-(*E*)-C(H)=C(H)Bu^t-10-(*E*)-C(H)=C(H)-Bu^t-7,8-$C_2B_9H_9$)] (**9**). The η^2 bonding mode of the 9-(*E*)-C(H)=C(H)Bu^t group to the metal is displaced in reactions with PMe_3, CNBu^t, and CO, yielding the species [Ru(CO)(PPh_3)(L)-(η^5-9,10-{(*E*)-C(H)=C(H)Bu^t}$_2$-7,8-$C_2B_9H_9$)] (L = PMe_3 (**10**), CNBu^t (**11**), CO (**12**)). The alkyne Me_3SiC≡CH reacts with **5** in the presence of traces of moisture to give [Ru(CO)(PPh_3)(η^2: η^5-9-C(H)=CH_2-7,8-$C_2B_9H_{10}$)] (**13**), having a molecular structure closely related to that of **8**, as confirmed by an X-ray diffraction study. Compound **13** reacts with CNBu^t to afford [Ru(CO)(PPh_3)(CNBu^t)(η^5-9-C(H)=CH_2-7,8-$C_2B_9H_{10}$)] (**14**), studied by X-ray diffraction, and with PMe_3 to give the ylide complex [Ru(CO)(PPh_3)(σ: η^5-9-C(H)(PMe_3)CH_2-7,8-$C_2B_9H_{10}$)] (**15**). The NMR data (^{1}H, ^{13}C{^{1}H}, ^{11}B{^{1}H}) are reported and discussed.

Introduction

We recently described a high-yield synthesis of the salt [K(18-crown-6)][RuH(PPh_3)$_2$(η^5-7,8-$C_2B_9H_{11}$)] and showed it to be a useful precursor to several new ruthenacarborane complexes.[1] In this paper we describe further studies on ruthenacarboranes having Ru(PPh_3)-(η^5-7,8-$C_2B_9H_{11}$) fragments. Molecules in which a ruthenium atom is part of a *closo*-3,1,2-RuC_2B_9 cage framework and where the metal also carries exopolyhedral ligands are of interest, because not only do they have counterparts in cyclopentadienide chemistry but they also undergo a variety of reactions involving both the associated ligands and the cage system.[2] Thus, the complex [Ru(CO)$_3$(η^5-7,8-$C_2B_9H_{11}$)],[2a] isolobal with [Ru-(CO)$_3$(η^5-C_5H_5)]$^+$ or [Mn(CO)$_3$(η^5-C_5H_5)], provides a route to many other species. These include reactions with alkynes RC≡CH, leading to replacement of BH cage vertexes with BC(H)=C(H)R groups,[2b] and reactions with metal−ligand fragments, affording bimetal complexes with exopolyhedral B−H⇀M bonds.[2a,c,e] Replacement of CO groups by phosphine ligands on the ruthenium in molecules with a *closo*-3,1,2-RuC_2B_9 core structure would be expected to influence the nature of products obtained by increasing electron density at the metal center. For this reason we have undertaken the examination of the chemistry of species containing Ru-(PPh_3)(η^5-7,8-$C_2B_9H_{11}$) fragments.

Results and Discussion

Treatment of Et_2O solutions of the salts [K(18-crown-6)][RuH(L)(PPh_3)(η^5-7,8-$C_2B_9H_{11}$)] (L = CO, PPh_3)[1] with HCl affords the complexes [K(18-crown-6)][RuCl(L)-

---

[†] The compounds described in this paper have a ruthenium atom incorporated into a *closo*-1,2-dicarba-3-ruthenadodecaborane framework. However, to avoid a complicated nomenclature for the complexes reported, and to relate them to the many known ruthenium species with η^5-coordinated cyclopentadienyl ligands, we treat the cages as *nido* 11-vertex ligands with numbering as for an icosahedron from which the 12th vertex has been removed.

(1) Ellis, D. D.; Couchman, S. M.; Jeffery, J. C.; Malget, J. M.; Stone, F. G. A. *Inorg. Chem.* **1999**, *38*, 2981.

(2) (a) Anderson, S.; Mullica, D. F.; Sappenfield, E. L.; Stone, F. G. A. *Organometallics* **1995**, *14*, 3516. (b) Anderson, S.; Mullica, D. F.; Sappenfield, E. L.; Stone, F. G. A. *Organometallics* **1996**, *15*, 1676. (c) Anderson, S.; Jeffery, J. C.; Liao, Y.-H.; Mullica, D. F.; Sappenfield, E. L.; Stone, F. G. A. *Organometallics* **1997**, *16*, 958. (d) Jeffery, J. C.; Jelliss, P. A.; Psillakis, E.; Rudd, G. E. A.; Stone, F. G. A. *J. Organomet. Chem.* **1998**, *562*, 17. (e) Jeffery, J. C.; Jelliss, P. A.; Rudd, G. E. A.; Sakanishi, S.; Stone, F. G. A.; Whitehead, J. *J. Organomet. Chem.* **1999**, *582*, 90.

10.1021/om000018i CCC: $19.00
Publication on Web 04/19/2000

Table 1. Analytical and Physical Data

compd	color	yield (%)	ν_{max}(CO)/ ν_{max}(NC)*[a] (cm^{-1})	anal. (%)[b] C	H
$[K(18\text{-crown-}6)][RuCl(CO)(PPh_3)(\eta^5\text{-}7,8\text{-}C_2B_9H_{11})]$ (**1**)	orange	90	1942 s	45.8 (46.0)	5.8 (5.8)
$[K(18\text{-crown-}6)][RuCl(PPh_3)_2(\eta^5\text{-}7,8\text{-}C_2B_9H_{11})]$ (**2**)	red	76		53.7 (54.8)	6.0 (6.0)
$[NEt_4][RuI(CO)(PPh_3)(\eta^5\text{-}7,8\text{-}C_2B_9H_{11})]$ (**3**)	red	92	1940 s	43.1 (43.0)	5.8 (5.8)[c,d]
$[Ru(CNBu^t)(CO)(PPh_3)(\eta^5\text{-}7,8\text{-}C_2B_9H_{11})]$ (**4**)	yellow	95	2166 s*, 1987 s	49.3 (49.0)	5.7 (5.6)[c,e]
$[Ru(CO)(PPh_3)\{\eta^2{:}\eta^5\text{-}9\text{-}(E)\text{-}C(H){=}C(H)Ph\text{-}7,8\text{-}C_2B_9H_{10}\}]$ (**8**)	orange	77	1972 s	54.7 (55.6)	5.2 (5.1)[f]
$[Ru(CO)(PPh_3)\{\eta^2{:}\eta^5\text{-}9\text{-}(E)\text{-}C(H){=}C(H)Bu^t\text{-}10\text{-}(E)\text{-}C(H){=}C(H)Bu^t\text{-}7,8\text{-}C_2B_9H_9\}]$ (**9**)	red	64	1963 s	57.3 (57.6)	6.7 (6.7)
$[Ru(CO)(PMe_3)(PPh_3)(\eta^5\text{-}9,10\text{-}\{(E)\text{-}C(H){=}C(H)Bu^t\}_2\text{-}7,8\text{-}C_2B_9H_9)]$ (**10**)	yellow	86	1959 s	56.3 (56.6)	7.3 (7.2)
$[Ru(CNBu^t)(CO)(PPh_3)(\eta^5\text{-}9,10\text{-}\{(E)\text{-}C(H){=}C(H)Bu^t\}_2\text{-}7,8\text{-}C_2B_9H_9)]$ (**11**)	yellow	84	2155 s*, 1987 s	59.3 (59.2)	7.3 (7.1)[g]
$[Ru(CO)_2(PPh_3)(\eta^5\text{-}9,10{-}\{(E)\text{-}C(H){=}C(H)Bu^t\}_2\text{-}7,8\text{-}C_2B_9H_9)]$ (**12**)	yellow	83	2002 s, 2049 s	57.5 (57.0)	6.6 (6.4)
$[Ru(CO)(PPh_3)\{\eta^2{:}\eta^5\text{-}9\text{-}C(H){=}CH_2\text{-}7,8\text{-}C_2B_9H_{10}\}]$ (**13**)	yellow	90	1973 s	50.3 (50.2)	5.1 (5.1)
$[Ru(CO)(PPh_3)(CNBu^t)\{\eta^5\text{-}9\text{-}C(H){=}CH_2\text{-}7,8\text{-}C_2B_9H_{10}\}]$ (**14**)	yellow	81	2160 s*, 1988 s	49.0 (48.5)	5.5 (5.4)[h,i]
$[Ru(CO)(PPh_3)\{\sigma{:}\eta^5\text{-}9\text{-}C(H)(PMe_3)CH_2\text{-}7,8\text{-}C_2B_9H_{10}\}]$ (**15**)	yellow	88	1906 s[j]	49.7 (49.9)	6.0 (5.9)

[a] Measured in CH_2Cl_2. A medium-intensity band observed at ca. 2550 cm^{-1} in the spectra of all compounds is due to B−H absorptions. [b] Calculated values are given in parentheses. [c] Crystallizes with half a molecule of CH_2Cl_2. [d] N 1.7 (1.7). [e] N 2.2 (2.2). [f] EI mass spectrum: *m/z* 625.96 ([**8**]$^+$) (calcd 625.26); 597.98 ([**8**]$^+$ − CO). [g] N 1.9 (1.8). [h] Crystallizes with a molecule of CH_2Cl_2. [i] N 2.0 (2.0). [j] Measured in Me_2CO.

Chart 1

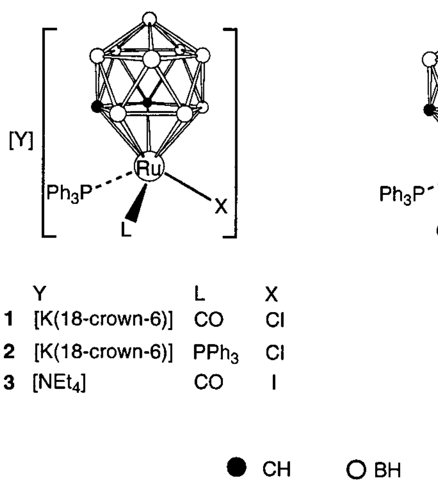

$(PPh_3)(\eta^5\text{-}7,8\text{-}C_2B_9H_{11})]$ (L = CO (**1**), PPh_3 (**2**); Chart 1) in yields which are essentially quantitative. The related iodo compound $[NEt_4][RuI(CO)(PPh_3)(\eta^5\text{-}7,8\text{-}C_2B_9H_{11})]$ (**3**) was prepared from the reaction between $[Ru(CO)(PPh_3)_2(\eta^5\text{-}7,8\text{-}C_2B_9H_{11})]$ and $[NEt_4]I$ in THF (tetrahydrofuran). The three compounds were characterized by the data given in Tables 1−3, but to place the structures of these species on a firm basis, that of **3** was established by a single-crystal X-ray diffraction study. The anion is shown in Figure 1 and is structurally akin to $[RuCl(CO)_2(\eta^5\text{-}7,8\text{-}C_2B_9H_{11})]^-$.[2a] Selected structural parameters are listed in Table 4. The anion adopts the "piano stool" structure with the ruthenium atom η^5-coordinated on one side by a *nido*-7,8-$C_2B_9H_{11}$ group and on the other by the CO, PPh_3, and I ligands (C−Ru−P = 91.1(2)°, P−Ru−I = 89.92(3)°, C−Ru−I = 92.4(2)°).

During the course of our studies it was observed that heating $[Ru(CO)(PPh_3)_2(\eta^5\text{-}7,8\text{-}C_2B_9H_{11})]$ with $CNBu^t$ in CH_2Cl_2 gave the complex $[Ru(CNBu^t)(CO)(PPh_3)(\eta^5\text{-}7,8\text{-}C_2B_9H_{11})]$ (**4**) by displacement of a PPh_3 group rather than a CO molecule from the ruthenium reactant.[1] This might be expected on both steric and electronic grounds. Data for **4** are reported in Tables 1−3. This is an early example of a molecule containing the target $Ru(CO)(PPh_3)(\eta^5\text{-}7,8\text{-}C_2B_9H_{11})$ fragment. However, the synthesis of the starting material, $[Ru(CO)(PPh_3)_2(\eta^5\text{-}7,8\text{-}C_2B_9H_{11})]$, necessitated an awkward synthetic procedure. Moreover our work established that the salt **1** was a more convenient precursor to new complexes.

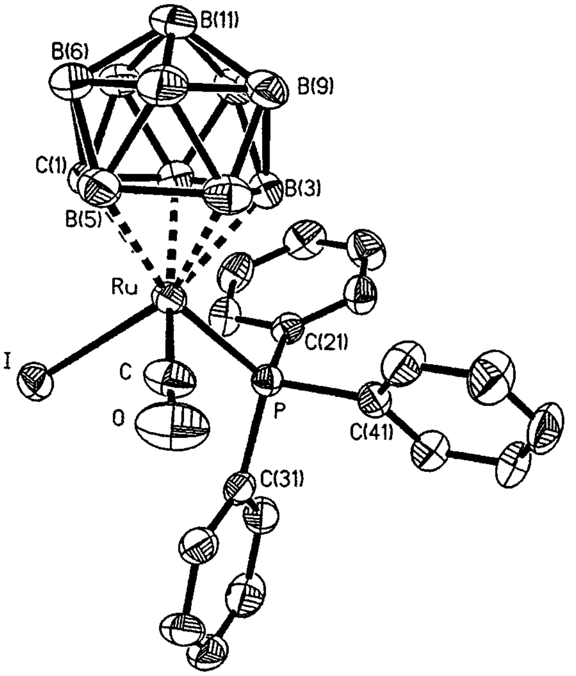

Figure 1. Structure of the anion of $[NEt_4][RuI(CO)(PPh_3)(\eta^5\text{-}7,8\text{-}C_2B_9H_{11})]$ (**3**), showing the crystallographic labeling scheme. Hydrogen atoms are omitted for clarity, and thermal ellipsoids are shown at the 40% probability level.

The presence of the labile THF molecule in the complex $[Ru(CO)_2(THF)(\eta^5\text{-}7,8\text{-}C_2B_9H_{11})]$[2a] makes it a very versatile synthon. Hence, it was of interest to establish whether the corresponding THF adduct could be derived from the species **1** when dissolved in THF, using $TlPF_6$ to remove halide. Although the desired species $[Ru(CO)(PPh_3)(THF)(\eta^5\text{-}7,8\text{-}C_2B_9H_{11})]$ (**5**) could not be isolated, spectroscopic studies on the yellow solutions formed in situ provided evidence for its formation. Thus, the solutions displayed in the IR a single CO absorption at ν_{max} 1964 cm^{-1}. The $^{11}B\{^1H\}$ NMR spectrum of **5** displays the expected nine signals, and the $^{31}P\{^1H\}$ NMR spectrum, measured in CD_2Cl_2 with a small amount of added THF, revealed a singlet at δ 48.0. The $^{31}P\{^1H\}$ NMR resonance for **1** is at δ 49.4, and that for **4** is at δ 46.5. When THF-d_8 was added to solutions of **5**, a second resonance slowly appeared at δ

Table 2. Hydrogen-1 and Carbon-13 NMR Data[a]

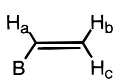

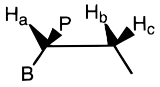

	$^1H/\delta$[b]	$^{13}C/\delta$[c]
1	1.89, 3.58 (br s × 2, 2 H, cage CH), 3.61 (m, 24 H, OCH_2), 7.26−7.74 (m, 15 H, Ph)	203.5 (d, CO, *J*(PC) = 21), 134.7−128.0 (Ph), 70.6 (OCH_2), 59.7, 41.3 (cage CH)
2	2.92 (br s, 2 H, cage CH), 3.58 (m, 24 H, OCH_2), 6.90−7.80 (m, 30 H, Ph)	139.1−126.8 (Ph), 70.5 (OCH_2), 45.7 (cage CH)
3	1.31 (t, 12 H, CH_2Me, *J*(HH) = 9), 1.65 (br s, 1 H, cage CH), 3.19 (q, 8 H, CH_2Me, *J*(HH) = 9), 4.11 (br s, 1 H, cage CH), 7.33−7.71 (m, 15 H, Ph)	204.8 (d, CO, *J*(PC) = 20), 134.6−127.8 (Ph), 53.2 (CH_2Me), 53.1, 38.7 (cage CH), 7.9 (CH_2Me)
4	1.26 (s, 9 H, Bu^t), 2.05, 2.15 (br s × 2, 2 H, cage CH), 7.46−7.49 (m, 15 H, Ph)	200.1 (d, CO, *J*(PC) = 15), 144.2 (br, $CNBu^t$), 133.6−129.3 (Ph), 58.8 (CMe_3), 46.0, 43.4 (cage CH), 30.3 (CMe_3)
8	0.70, 3.09 (br s × 2, 2 H, cage CH), 3.89 (d of d, 1 H, ═C*H*Ph, *J*(HH) = 13, *J*(PH) = 5), 5.16 (d, 1 H, ═CHB, *J*(HH) = 13), 6.92−7.42 (m, 20 H, Ph)	198.6 (d, CO, *J*(PC) = 20), 139.2−126.3 (Ph), 82.0 (br, ═CHB), 81.0 (═*C*HPh), 61.3, 37.8 (cage CH)
9	−0.25 (br s, 1 H, cage CH), 0.83, 1.02 (s × 2, 18 H, Bu^t), 2.95 (br s, 1 H, cage CH),[d] 4.06 (br s, 1 H, ═CHB),[d] 4.76 (d, 1 H, ═C*H*Bu^t, *J*(HH) = 14), 5.67, 5.95 (d × 2, 2 H, ═CHB and ═C*H*Bu^t, *J*(HH) = 18, 18], 7.42−7.63 (m, 15 H, Ph)	201.1 (d, CO, *J*(PC) = 18), 147.3,[d] 133.3 (═*C*HBu^t), 131.1−129.2 (Ph), 105.2,[d] 87.3 (br, ═CHB), 58.1, 35.3 (br, cage CH), 34.7, 34.2 (CMe_3), 31.5, 29.7 (CMe_3)
10	0.98, 1.10 (s × 2, 18 H, Bu^t), 1.22 (d, 9 H, PMe_3, *J*(PH) = 9), 3.35, 3.33 (br s × 2, 2 H, cage CH), 5.65, 5.77, 5.85, 6.32 (d × 4, 4 H, ═C*H*Bu^t × 2 and ═CHB × 2, *J*(HH) = 17, 17, 17, 17), 7.39−7.59 (m, 15 H, Ph)	204.6 (d of d, CO, *J*(PC) = 16, 19), 149.4, 147.6 (═CHBu^t), 135.1, 134.6 (br, ═CHB), 134.1−128.6 (Ph), 51.3 (cage CH), 36.5, 34.3 (CMe_3), 30.8 (cage CH), 30.0, 29.6 (CMe_3), 19.2 (d, MeP, *J*(PC) = 30)
11	1.03, 1.07, 1.20 (s × 3, 27 H, Bu^t), 1.42, 3.32 (br s × 2, 2 H, cage CH), 5.66, 5.72, 5.73, 6.09 (d × 4, 4 H, ═C*H*Bu^t × 2 and ═CHB × 2, *J*(HH) = 18, 18, 18, 18), 7.43−7.59 (m, 15 H, Ph)	202.5 (d, CO, *J*(PC) = 16), 146.3, 146.0 (═CHBu^t), 145.0 (br, $CNBu^t$), 133.7−128.9 (Ph), 131.8 (br, ═CHB), 127.6 (br, ═CHB), 58.5, 51.3 (cage CH), 51.2 ($NCMe_3$), 39.6, 34.1 (CMe_3), 30.2, 30.1, 29.8 (CMe_3)
12	0.97, 1.02 (s × 2, 18 H, Bu^t), 1.93, 2.37 (br s × 2, 2 H, cage CH), 5.56, 5.74, 5.76, 5.83 (d × 4, 4 H, ═C*H*Bu^t × 2, and ═CHB × 2, *J*(HH) = 18, 18, 18, 18), 7.49−7.56 (m, 15 H, Ph)	198.4, 196.0 (d × 2, CO, *J*(PC) = 15, 15), 147.7, 146.4 (═CHBu^t), 133.3−128.7 (Ph),[e] 128.8 (vbr, ═CHB), 47.1, 45.8 (cage CH), 34.1, 29.3 (CMe_3), 29.9, 29.2 (CMe_3)
13	0.18 (br s, 1 H, cage CH), 2.05 (d of d, 1 H, $=CH_bH_c$, $J(H_aH_c)$ = 13, *J*(PH) = 6), 3.05 (br s, 1 H, cage CH), 3.70 (d, 1 H, $=CH_bH_c$, $J(H_aH_b)$ = 9), 4.71 (d of d, 1 H, $=CH_aB$, $J(H_cH_a)$ = 13, $J(H_bH_a)$ = 9), 7.46−7.56 (m, 15 H, Ph)	198.4 (d, CO, *J*(PC) = 20), 133.4−129.2 (Ph), 81.9 (br, ═CHB), 60.7 (d, $=CH_2$, *J*(PC) = 3), 60.2, 39.7 (cage CH)
14	1.19 (s, 9 H, Bu^t), 1.61, 3.42 (br s × 2, 2 H, cage CH), 5.10 (d of d, 1 H, $=CH_bH_c$, $J(H_aH_b)$ = 13, $J(H_cH_b)$ = 4), 5.16 (d of d, 1 H, $=CH_bH_c$, $J(H_aH_c)$ = 19, $J(H_bH_c)$ = 4), 6.17 (d of d, 1 H, $=CH_aB$, $J(H_cH_a)$ = 19, $J(H_bH_a)$ = 13), 7.45−7.56 (m, 15 H, Ph)	201.9 (d, CO, *J*(PC) = 16), 145.7 (br, ═CHB), 143.8 ($CNBu^t$), 133.7−128.9 (Ph), 118.4 ($=CH_2$), 58.5 (CMe_3), 51.5 (d, cage CH, *J*(PC) = 9), 41.5 (cage CH), 30.1 (CMe_3)
15[f]	0.40 (br s, 1 H, cage CH), 1.18 (d of d, 1 H, CH_bH_c, $J(H_aH_b)$ = 9, *J*(PH) = 9), 1.33 (d, 9 H, Me, *J*(PH) = 14), 1.53 (d, 1 H, CH_bH_c, $J(H_aH_c)$ = 15), 2.18 (d of d of d, 1 H, CH_aBP, $J(H_cH_a)$ = 15, $J(H_bH_a)$ = 9, *J*(PH) = 9), 2.39 (br s, 1 H, cage CH), 7.45−7.53 (m, 15 H, Ph)	206.5 (d, CO, *J*(PC) = 20), 134.7−128.4 (Ph), 47.2, 30.4 (cage CH), 22.7 (br, *C*HB), 18.1 (CH_2), 5.9 (d, PMe_3, *J*(PC) = 53)

[a] Units and conditions: chemical shifts (δ) in ppm; coupling constants (*J*) in Hz; measurements in CD_2Cl_2 as solvent, unless otherwise stated. [b] Resonances for terminal B−H protons occur as broad unresolved signals in the range ca. −2 to 3. [c] Hydrogen-1 decoupled; chemical shifts are positive to high frequency of $SiMe_4$. [d] Signals assigned to η^2-C(H)═C(H)Bu^t group ligating the Ru atom. [e] Two separate signals expected; peaks not resolved due to proximity and broadness. [f] Recorded in $(CD_3)_2SO$ due to insolubility of the complex.

47.4 which increased in intensity upon further addition of deuterated solvent. This suggests a facile exchange between THF and THF-d_8 at the ruthenium center.

We have previously reported reactions between [$Ru(CO)_2(THF)(\eta^5\text{-}7,8\text{-}C_2B_9H_{11})$] and alkenes and alkynes (RC≡CH and RC≡CR′, R, R′ = alkyl, aryl).[2b,d] Alkenes, as well as internal alkynes of the type RC≡CR′, afford stable η^2 complexes of formulation [$Ru(CO)_2$(alkene or alkyne)(η^5-7,8-$C_2B_9H_{11}$)]. However, terminal alkynes, RC≡CH, give ruthenium-cage substitution products with η^2-(*E*)-BC(H)═C(H)R groups; e.g., in a reaction between [$Ru(CO)_2(THF)(\eta^5\text{-}7,8\text{-}C_2B_9H_{11})$] and an excess of Bu^tC≡CH the compound [$Ru(CO)_2$(η^2:η^5-9-(*E*)-C(H)═C(H)Bu^t-10,11-{(*E*)-C(H)═C(H)Bu^t}$_2$-7,8-$C_2B_9H_8$)] (**6**; Chart 2) was formed. We were prompted by these results to investigate reactions of **5** with both alkenes and alkynes. For these experiments **5** was generated from **1** as described above and used in situ because of its lability.

In contrast with [$Ru(CO)_2(THF)(\eta^5\text{-}7,8\text{-}C_2B_9H_{11})$], which upon treatment with $Me_3SiCH=CH_2$ afforded the stable complex [$Ru(CO)_2(Me_3SiCH=CH_2)(\eta^5\text{-}7,8\text{-}C_2B_9H_{11})$],[2b] the alkene did not react with THF solutions of **5**. However, bubbling C_2H_4 through THF solutions yielded, after separation by column chromatography, an unstable yellow solid identified spectroscopically as [$Ru(CO)(PPh_3)(C_2H_4)(\eta^5\text{-}7,8\text{-}C_2B_9H_{11})$] (**7**). The IR spectrum showed a single CO stretch at 1991 cm^{-1}, to be compared with that observed at 1964 cm^{-1} in the solutions of **5**. The coordinated C_2H_4 molecule was revealed in the ^1H NMR spectrum by a multiplet at δ ca. 3.22 and in the $^{13}C\{^1H\}$ NMR spectrum by a doublet at δ 61.0 (*J*(PC) = 13 Hz). The corresponding signals in the spectra of [$Ru(CO)_2(C_2H_4)(\eta^5\text{-}7,8\text{-}C_2B_9H_{11})$] are seen at δ 3.80 ($^1H$) and 64.6 ($^{13}C$).[2b] The $^{31}P\{^1H\}$ NMR spectrum of **7** shows a singlet peak at δ 54.4. It is evident from these studies that the fragment $Ru(CO)(PPh_3)(\eta^5\text{-}7,8\text{-}C_2B_9H_{11})$ bonds alkenes less tightly than does $Ru(CO)_2(\eta^5\text{-}7,8\text{-}C_2B_9H_{11})$, perhaps due to reduced electrophilicity at the Ru center when CO is replaced by PPh_3. Similar behavior was observed in reactions with alkynes RC≡CR. Thus, whereas it was possible to isolate the stable compound

Table 3. Boron-11 and Phosphorus-31 NMR Data[a]

	^{11}B/δ[b]	^{31}P/δ[c]
1	−2.2 (1 B), −6.6 (2 B), −9.6 (1 B), −12.6 (1 B), −16.0 (1 B), −19.5 (1 B), −21.9 (1 B), −25.7 (1 B)	49.4
2	−2.2 (1 B), −6.3 (2 B), −10.5 (1 B), −13.4 (3 B), −26.1 (2 B)	38.5
3	−1.4 (1 B), −6.5 (3 B), −13.8 (1 B), −15.9 (1 B), −18.4 (1 B), −22.4 (1 B), −24.5 (1 B)	51.1
4	0.5 (1 B), −5.5 (1 B), −7.7 (1 B), −8.6 (1 B), −9.8 (2 B), −21.1 (3 B)	46.5
8	7.9 (1 B), 6.6 (1 B), 1.6 (2 B), −14.0 (1 B), −15.6 (1 B), −18.6 (1 B), −21.6 (2 B)	40.0
9	16.0 (1 B, B−C), 8.3 (1 B, B−C), 3.6 (1 B), 1.3 (1 B), −13.5 (1 B), −15.8 (1 B), −19.6 (1 B), −23.4 (2 B)	41.3
10	9.3 (1 B, B−C), 0.0 (1 B), −1.8 (1 B), −4.8 (1 B, B−C), −9.0 (1 B), −11.9 (1 B), −18.5 (2 B), −26.2 (1 B)	46.6 (d, PPh$_3$, *J*(PP) = 31), −9.7 (d, PMe$_3$, *J*(PP) = 31)
11	8.7 (1 B, B−C), −1.3 (1 B), −2.7 (2 B), −10.2 (2 B), −17.5 (1 B), −19.6 (1 B), −25.0 (1 B)	47.3
12	7.6 (1 B, B−C), 2.5 (2 B), −4.5 (2 B), −9.1 (1 B), −16.1 (1 B), −20.3 (1 B), −24.0 (1 B)	41.4
13	9.2 (1 B, B−C), 6.3 (1 B), 1.2 (2 B), −13.1 (1 B), −15.2 (1 B), −19.2 (1 B), −21.4 (2 B)	46.3
14	0.1 (1 B), −2.1 (1 B),[d] −4.5 (2 B, B−C), −9.4 (1 B), −11.7 (1 B), −17.6 (1 B), −19.1 (1 B), −22.7 (1 B)	50.9
15[e]	−6.5 (3 B), −9.5 (2 B), −12.4 (2 B), −21.0 (1 B), −25.1 (1 B)	50.9 (PPh$_3$), 24.2 (PMe$_3$)

[a] Units and conditions: chemical shifts (δ) in ppm; coupling constants (*J*) in Hz; measurements in CD_2Cl_2 as solvent. [b] Hydrogen-1 decoupled; chemical shifts are positive to high frequency of $BF_3 \cdot Et_2O$ (external). Peaks due to B−C boron nuclei were identified as singlets in the fully coupled ^{11}B NMR spectrum. Those in complexes **8** and **15**, and one each in **11** and **12**, could not be unambiguously assigned. [c] Hydrogen-1 decoupled; chemical shifts are positive to high frequency of H_3PO_4 (external). [d] Single B−C boron resonance overlaps with a B−H boron signal. [e] Recorded in $(CD_3)_2SO$.

Table 4. Selected Internuclear Distances (Å) and Angles (deg) for [NEt$_4$][RuI(CO)(PPh$_3$)(η^5-7,8-C$_2$B$_9$H$_{11}$)]·CH$_2$Cl$_2$ (3)

Ru−P	2.3243(12)	Ru−I	2.7574(6)	Ru−B(4)	2.267(5)	Ru−C	1.842(6)
Ru−C(1)	2.246(5)	Ru−C(2)	2.246(5)	Ru−B(5)	2.290(6)	Ru−B(3)	2.219(6)
P−C(41)	1.842(5)	P−C(21)	1.836(4)	P−C(31)	1.843(5)	C−O	1.142(6)
C−Ru−P	91.1(2)	C−Ru−I	92.4(2)	O−C−Ru	174.1(5)	P−Ru−I	89.92(3)

Chart 2

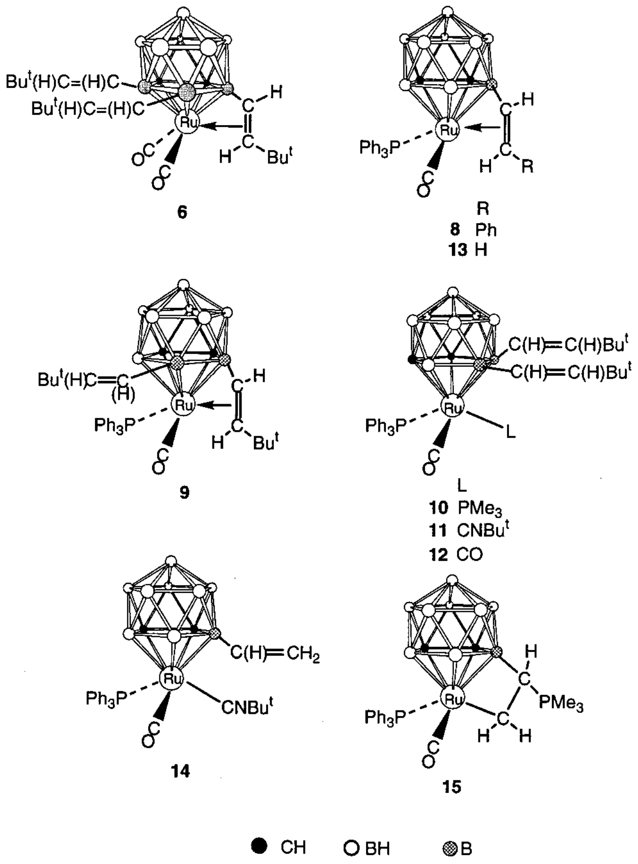

[Ru(CO)$_2$(MeC≡CMe)(η^5-7,8-C$_2$B$_9$H$_{11}$)],[2b] the related species [Ru(CO)(PPh$_3$)(MeC≡CMe)(η^5-7,8-C$_2$B$_9$H$_{11}$)] appears to have only a fleeting existence. Only when **5** was treated with a 10-fold excess of MeC≡CMe, and when CH$_2$Cl$_2$ was used as solvent instead of THF, was there any evidence for the formation of the but-2-yne complex [Ru(CO)(PPh$_3$)(MeC≡CMe)(η^5-7,8-C$_2$B$_9$H$_{11}$)]. This evidence rests on the appearance of a CO band in the IR spectrum at 1989 cm^{-1} and a resonance in the ^{31}P{^{1}H} NMR spectrum at δ 42.6. Removal of MeC≡CMe from the solutions or chromatography of the mixture resulted in decomposition.

Although **5** displayed little propensity to react with disubstituted alkynes RC≡CR, monosubstituted alkynes RC≡CH readily reacted. Thus, [Ru(CO)(PPh$_3$)(η^2: η^5-9-(*E*)-C(H)=C(H)Ph-7,8-C$_2$B$_9$H$_{10}$)] (**8**) was obtained when a 3-fold excess of PhC≡CH was employed in reactions with **1** in THF to which TlPF$_6$ had been added. Data for **8** are summarized in Tables 1−3. An X-ray crystallographic analysis was carried out to establish the structure fully, since NMR data alone (vide infra) could not conclusively determine to which boron atom in the $\overline{\text{CCBBB}}$ ring the η^2-(*E*)-C(H)=C(H)Ph fragment was attached. The results are summarized in Table 5, and the molecule is shown in Figure 2. The ruthenium atom is η^5-coordinated by the open face of the *nido*-7,8-C$_2$B$_9$ cage, as expected. However, the metal atom is also η^2-coordinated by a C=C bond of the *trans*-BC(H)=C(H)-Ph group which is attached to a boron atom lying in an α-site with respect to the carbons of the $\overline{\text{CC}\mathit{B}\text{BB}}$ ring ligating the ruthenium. The structure has a strong resemblance to that of [Ru(CO)$_2$(η^2:η^5-9-(*E*)-C(H)=C(H)-Bu^t-7,8-C$_2$B$_9$H$_{10}$)] obtained from [Ru(CO)$_2$(THF)(η^5-7,8-C$_2$B$_9$H$_{11}$)] and Bu^{t}C≡CH when 1 equiv of the alkyne is used for reaction.[2b] However, as mentioned above and further discussed below, when 3 equiv of Bu^{t}C≡CH is employed in the reaction with [Ru(CO)$_2$(THF)(η^5-7,8-C$_2$B$_9$H$_{11}$)], the product is exclusively **6**. In the molecule **8** the C(4)−C(5) (1.404(5) Å), Ru−C(4) (2.221(4) Å), Ru−C(5) (2.397(4) Å), and Ru−B(3) (2.144(4) Å) distances are essentially the same as those of the corresponding connectivities in [Ru(CO)$_2$(η^2:η^5-9-(*E*)-C(H)=C(H)Bu^t-7,8-C$_2$B$_9$H$_{10}$)] (1.398(7), 2.249(6), 2.401(5), and 2.152(6)

Table 5. Selected Internuclear Distances (Å) and Angles (deg) for $[Ru(CO)(PPh_3)\{\eta^2:\eta^5\text{-}9\text{-}(E)\text{-}C(H){=}C(H)Ph\text{-}7,8\text{-}C_2B_9H_{10}\}]$ (8)

Ru−C(3)	1.844(4)	Ru−B(3)	2.144(4)	Ru−C(4)	2.221(4)	Ru−C(2)	2.227(3)
Ru−C(1)	2.277(4)	Ru−B(4)	2.296(4)	Ru−B(5)	2.319(4)	Ru−P	2.3746(10)
Ru−C(5)	2.397(4)	B(3)−C(4)	1.510(6)	C(3)−O(3)	1.143(4)	C(4)−C(5)	1.404(5)
C(5)−C(41)	1.467(5)						
C(3)−Ru−B(3)	123.5(2)	O(3)−C(3)−Ru	175.4(3)	C(4)−Ru−B(5)	116.6(2)	C(3)−Ru−C(1)	132.9(2)
C(3)−Ru−C(2)	166.50(14)	C(4)−C(5)−Ru	65.6(2)	C(3)−Ru−C(5)	104.5(2)	C(4)−Ru−B(4)	73.7(2)
C(4)−Ru−C(1)	114.6(2)	C(3)−Ru−C(4)	102.2(2)	C(5)−C(4)−B(3)	123.9(4)	C(3)−Ru−P	89.03(12)
C(3)−Ru−B(5)	94.4(2)	C(4)−Ru−C(2)	76.24(14)	C(41)−C(5)−Ru	126.6(2)	P−Ru−C(5)	90.14(9)
C(4)−Ru−P	125.28(10)	C(3)−Ru−B(4)	87.7(2)	B(3)−Ru−C(4)	40.4(2)	C(5)−C(4)−Ru	79.3(2)

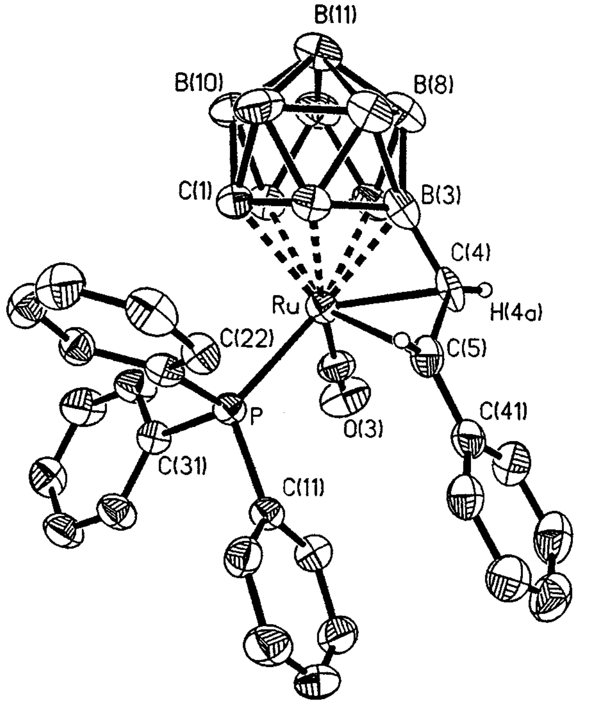

Figure 2. Structure of $[Ru(CO)(PPh_3)(\eta^2\text{: }\eta^5\text{-}9\text{-}(E)\text{-}C(H){=}C(H)Ph\text{-}7,8\text{-}C_2B_9H_{10})]$ (**8**), showing the crystallographic labeling scheme. Except for H(4a) and H(5a), hydrogen atoms are omitted for clarity, and thermal ellipsoids are shown at the 40% probability level.

Å). Interestingly, the formation of $[Ru(CO)_2(\eta^2\text{:}\eta^5\text{-}9\text{-}(E)\text{-}C(H){=}C(H)Bu^t\text{-}7,8\text{-}C_2B_9H_{10})]$ is accompanied by that of its isomer $[Ru(CO)_2(\eta^2\text{:}\eta^5\text{-}10\text{-}(E)\text{-}C(H){=}C(H)Bu^t\text{-}7,8\text{-}C_2B_9H_{10})]$, as revealed by NMR spectroscopy.[2b] In contrast with the reaction of **5** with PhC≡CH, we found no evidence for an isomer of **8** with the η^2-(*E*)-C(H)=C(H)Ph group attached to the β-boron (or 10-position) in the CCB*B*B coordinating face.

The NMR data for **8** are in agreement with the results of the X-ray diffraction study. Because of the high degree of asymmetry of the *nido*-7,8-C_2B_9 framework there are two widely separated resonances in the ^1H and in the $^{13}C\{^1H\}$ NMR spectra (Table 2) for the cage CH groups (^1H, δ 0.70 and 3.09; $^{13}C\{^1H\}$, δ 37.8 and 61.3). The signals for the protons of the η^2-9-(*E*)-C(H)=C(H)-Ph group display a $^1H-^1H$ coupling of 13 Hz, this value being in accord with their transoid arrangement. The signal at δ 3.89 shows a small doublet coupling of 5 Hz. This was shown to be due to the ^{31}P nucleus of the coordinated phosphine ligand, as it disappeared in a $^1H\text{-}\{^{31}P\}$ spectrum. In the $^{11}B\{^1H\}$ and ^{11}B NMR spectra, a peak could not be unambiguously accredited to the B−C boron nucleus, due to apparent overlap with another signal. However this α-boron is likely to resonate at δ 1.6, because the remaining signals (Table 3) all appear as doublets in the fully coupled ^{11}B NMR spectrum and because these resonances usually appear toward the low-field end of the spectrum.[3]

The reaction between **1** and a 3-fold excess of $Bu^tC{\equiv}CH$ in THF at room temperature, in the presence of $TlPF_6$, was next investigated. Column chromatography of the mixture afforded the complex $[Ru(CO)(PPh_3)\text{-}(\eta^2\text{: }\eta^5\text{-}9\text{-}(E)\text{-}C(H){=}C(H)Bu^t\text{-}10\text{-}(E)\text{-}C(H){=}C(H)Bu^t\text{-}7,8\text{-}C_2B_9H_9)]$ (**9**), identified by the data listed in Tables 1−3. To establish the site of attachment of the C(H)=C(H)-Bu^t groups to the cage borons, a single-crystal X-ray diffraction study was undertaken. The crystals were small and poorly diffracting, precluding a satisfactory analysis; hence, the results are provided in the Supporting Information. Nevertheless, the data could be analyzed sufficiently to establish firmly that one C(H)=C(H)Bu^t group is linked to a boron lying in an α-site in the CC*B*BB ring with this alkenyl group η^2-bonded to the ruthenium atom, while a second C(H)=C(H)Bu^t group is bonded to a cage boron which is at a β-site and is pendant.

The presence of the two *trans*-C(*H*)=C(*H*)Bu^t protons in **9** is evident from the ^1H NMR spectrum (Table 2), with the display of two pairs of signals at δ 4.06 and 4.76 and at δ 5.67 and 5.95. Since the former pair are at higher field, they are assigned to the C(H)=C(H)Bu^t moiety coordinated to the ruthenium atom.[2b] The signal at δ 4.06 actually appears as a very broad signal, likely due to the nearby quadrupolar boron nucleus. To confirm that this was indeed due to the =CHB proton, a $^1H-^1H$ COSY NMR spectrum (Figure 3) was measured. An off-diagonal correlation with the resonance at δ 4.76 satisfies this assignment, and a correlation between the doublets at δ 5.67 and 5.95 is also clearly evident. Diagnostic peaks for the carbons of the *C*(H)=*C*(H)Bu^t groups are seen in the $^{13}C\{^1H\}$ NMR spectrum at δ 147.3 and 133.3 and at δ 105.2 and 87.3. The last two resonances are characteristically broad, as is usual for carbon nuclei attached to boron atoms.[3] Resonances for the cage CH groups are observed in both the ^1H (δ −0.25 and 2.95) and $^{13}C\{^1H\}$ (δ 58.1 and 35.3) NMR spectra, the widely disparate chemical shifts being indicative of the degree of asymmetry of the *nido*-9,10-$\{C(H){=}C(H)Bu^t\}_2\text{-}7,8\text{-}C_2B_9H_9$ framework in addition to the chirality at ruthenium. The $^{11}B\{^1H\}$ NMR spectrum (Table 3) shows eight signals, one peak being broad and corresponding in intensity to two boron nuclei. The

---

(3) Brew, S. A.; Stone, F. G. A. *Adv. Organomet. Chem.* **1993**, *35*, 135,

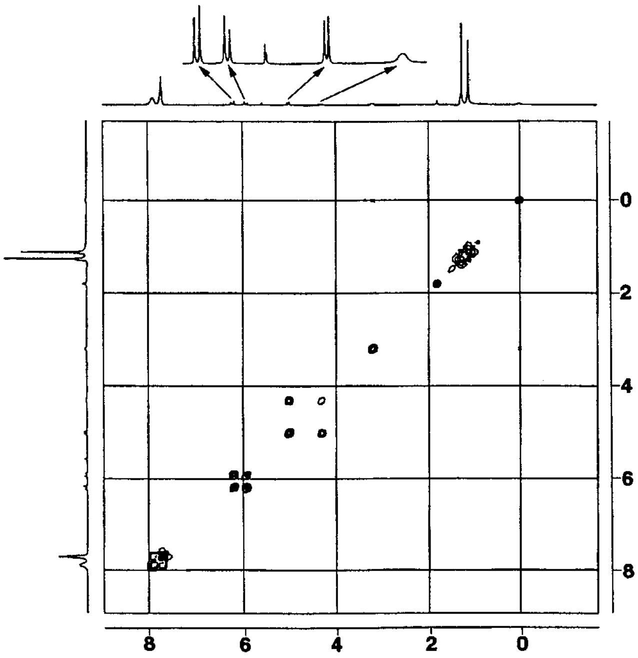

Figure 3. 360.13 MHz ^{1}H−^{1}H COSY NMR spectrum of compound **9**.

resonances at δ 8.3 and 16.0 may be ascribed to the *B*C(H)═C(H)Bu^t nuclei, on the basis of their chemical shift and their appearance as singlets in a fully coupled ^{11}B spectrum.[3]

In the reaction between **5** and Bu^{t}C≡CH there was no evidence for formation of a product with three BC(H)═C(H)Bu^t groups linked to the cage as occurs in **6**. Evidently for electronic or steric reasons the replacement of a CO molecule in the fragment Ru(CO)$_2$(η^5-7,8-C$_2$B$_9$H$_{11}$) by a PPh$_3$ group inhibits the pathway by which the trisubstituted cage would be formed. It seems probable that displacement of the η^2-9-(*E*)-BC(H)═C(H)-Bu^t group in **9** by a third molecule of Bu^{t}C≡CH to afford the intermediate [Ru(CO)(PPh$_3$)(η^2-Bu^{t}C≡CH)(η^5-9,10-{C(H)═C(H)Bu^t}$_2$-7,8-C$_2$B$_9$H$_9$)] would be a necessary step toward introducing a third BC(H)═C(H)Bu^t group. Conversion of this intermediate into a product akin to **6** but with an Ru(CO)(PPh$_3$) group would then follow. Although complexes [Ru(CO)(PPh$_3$)(η^2-RC≡CH)(η^5-7,8-C$_2$B$_9$H$_{11}$)] (R = Ph, Bu^t) were not isolated in the reactions which afford **8** and **9**, it is reasonable to assume that they are involved along the reaction pathway. With a large excess of RC≡CH the η^2-alkyne complex could be present in minor amounts in equilibrium with **5**, and this equilibrium is carried forward on formation of a BC(H)═C(H)R group, allowing the reaction to proceed to the end products.

It was of interest to determine whether the η^2 bonding mode of the ruthenium-coordinated C(H)═C(H)Bu^t group in **9** could be lifted by treatment of the complex with donor molecules. It has been previously shown that **6** reacts with PMe$_3$ to give [Ru(CO)$_2$(PMe$_3$)(η^5-9,10,11-{C(H)═C(H)Bu^t}$_3$-7,8-C$_2$B$_9$H$_8$)].[2b] Solutions of **9** reacted with PMe$_3$, CNBu^t, and CO to afford the compounds [Ru(L)(CO)(PPh$_3$)(η^5-9,10-{(*E*)-C(H)═C(H)Bu^t}$_2$-7,8-C$_2$B$_9$H$_9$)] (L = PMe$_3$ (**10**), CNBu^t (**11**), CO (**12**)), characterized by the information given in Tables 1−3. The NMR data for these structurally similar molecules are in accord with their formulations. Thus, the ^{1}H and ^{13}C{^{1}H} NMR spectra (Table 2) show the expected resonances for the two *trans*-BC(H)═C(H)Bu^t groups in different environments, except in the case of the ^{13}C{^{1}H} spectrum of **12** only one very broad ═CHB peak is seen, due to the proximity of two signals and nearness of ^{11}B nuclei. For **10** the ^{11}B{^{1}H} NMR spectrum was well-resolved, leading to an unambiguous assignment of the two resonances for the ═CHB nuclei from a fully coupled ^{11}B spectrum. However, for **11** and **12** only one of each pair of these ^{11}B signals could be identified (Table 3).

Earlier we reported that the reaction between Me$_3$SiC≡CH and [Ru(CO)$_2$(THF)(η^5-7,8-C$_2$B$_9$H$_{11}$)] yielded a mixture of isomers of the complexes [Ru(CO)$_2$(η^2:η^5-*n*-(*E*)-C(H)═C(H)SiMe$_3$-7,8-C$_2$B$_9$H$_{10}$] and [Ru(CO)$_2$(η^2:η^5-*n*-C(H)═CH$_2$-7,8-C$_2$B$_9$H$_{10}$] (n = 9, 10). In this mixture the isomers resulting from cleavage of SiMe$_3$ groups largely predominated.[2b] It was therefore of interest to investigate the corresponding reaction between **5** and Me$_3$SiC≡CH. The product isolated was [Ru(CO)(PPh$_3$)(η^2: η^5-9-C(H)═CH$_2$-7,8-C$_2$B$_9$H$_{10}$)] (**13**), formed as a single isomer. Evidently facile cleavage of the Me$_3$Si group occurred as in the reaction of the alkyne with [Ru(CO)$_2$(THF)(η^5-7,8-C$_2$B$_9$H$_{11}$)], though the reaction of **5** is more regioselective with respect to substitution by the organic fragment on the $\overline{\text{CCBBB}}$ face.

Although it was apparent from the limited number of peaks in the NMR spectra of complex **13** that it was formed as a single isomer, an X-ray diffraction study was carried out to establish the precise position of attachment of the vinyl group to the cage. The results confirmed that the isomer formed was indeed the 9-C(H)═CH$_2$-7,8-C$_2$B$_9$H$_{10}$ species. However, the X-ray data were so similar to those of **8** that they are included in the Supplementary Information. Peaks in the NMR spectra of **13** are as expected (Tables 2 and 3). The ^{1}H and ^{13}C{^{1}H} NMR spectra show resonances for the cage CH groups at δ 0.18 and 3.05 and at δ 60.2 and 39.7, respectively. In each pair of signals the chemical shifts are disparate, as expected because of the highly asymmetric cage structure. Resonances for the BC(H)═CH$_2$ group are also readily apparent in the ^{1}H and ^{13}C{^{1}H} spectra, while in the ^{11}B{^{1}H} spectrum one peak (δ 9.2) remained a singlet in a fully coupled ^{11}B spectrum and can thus be assigned to the ═CHB group.

It is likely that traces of water either in the glassware or present in the solvents, although the latter were vigorously dried, are responsible for cleavage of the silyl group observed in the formation of **13**. This feature has been observed previously by others[4−6] and by us.[7] In our system traces of water would convert the initially formed alkyne η^2-complex [Ru(CO)(PPh$_3$)(Me$_3$SiC≡CH)(η^5-7,8-C$_2$B$_9$H$_{11}$)] into [Ru(CO)(PPh$_3$)(HC≡CH)(η^5-7,8-C$_2$B$_9$H$_{11}$)]. Rearrangement of the latter to the vinylidene complex [Ru(═C═CH$_2$)(CO)(PPh$_3$)(η^5-7,8-C$_2$B$_9$H$_{11}$)] would

---

(4) Knaup, W.; Werner, H. *J. Organomet. Chem.* **1991**, *411*, 471. Höhn, A.; Otto, H.; Dziallis, M.; Werner, H. *J. Chem. Soc., Chem. Commun.* **1987**, 852. Höhn, A.; Werner, H. *J. Organomet. Chem.* **1990**, *382*, 255.

(5) Espuelas, J.; Esteruelas, M. A.; Lahoz, F. J.; Oro, L. A.; Ruiz, N. *J. Am. Chem. Soc.* **1993**, *115*, 4683.

(6) Buil, M. L.; Eisenstein, O.; Esteruelas, M. A.; García-Yebra, C.; Gutiérrez-Puebla, E.; Oliván, M.; Oñate, E.; Ruiz, N. Tajada, M. A. *Organometallics* **1999**, *18*, 4949.

(7) Dossett, S. J.; Li, S.; Mullica, D. F.; Sappenfield, E. L.; Stone, F. G. A. *J. Chem. Soc., Dalton Trans.* **1993**, 3551.

then take place, and this would be followed by insertion into a BH vertex in the α-site in the $\overline{\mathrm{CC}B\mathrm{BB}}$ ring ligating the ruthenium to give **13**. A similar pathway proceeding through the well-established[8,9] process of an initially formed η^2-alkyne−metal complex transforming into a vinylidene−metal species would also account for the formation of **8** and **9**. It has been noted[6] that the π-alkyne−vinylidene isomerization is more favored for $Bu^tC{\equiv}CH$ and $Me_3SiC{\equiv}CH$ than it is for $PhC{\equiv}CH$. This may account for the reaction between **5** and $PhC{\equiv}CH$ giving **8** having one C(H)=C(H)Ph group, whereas $Bu^tC{\equiv}CH$ gives **9** with two $C(H){=}C(H)Bu^t$ groups. However, only one $C(H){=}CH_2$ group is present in **13** so that other factors beside the π-alkyne−vinylidene rearrangement must be important; no doubt the steric and electronic requirements of the PPh_3 ligand play a part.

To demonstrate the importance of water in the formation of **13**, a small quantity of D_2O was added to the mixture containing **1** in THF with $TlPF_6$ before treatment with $Me_3SiC{\equiv}CH$. Workup of the product, as in the synthesis of **13**, led to the isolation of a 1:1 mixture of the two isomers $[Ru(CO)(PPh_3)(\eta^2{:}\eta^5\text{-}9\text{-}(Z)\text{-}C(H){=}C(H)D\text{-}7,8\text{-}C_2B_9H_{10})]$ (**13a**) and $[Ru(CO)(PPh_3)(\eta^2{:}\eta^5\text{-}9\text{-}(E)\text{-}C(H){=}C(H)D\text{-}7,8\text{-}C_2B_9H_{10})]$ (**13b**) (Scheme 1). Structural assignments for the isomers were made from the $^{13}C\{^1H\}$, ^1H, and ^2H NMR spectra of the mixture. Comparison of the $^{13}C\{^1H\}$ NMR spectrum of **13a,b** with that of the nondeuterated compound **13** showed that the peak at δ 60.7 becomes a somewhat broad triplet with $J(^2HC) = 25$ Hz, confirming that only one D atom is bound to this carbon. The ^2H NMR spectrum (Supporting Information) displays two signals at δ 3.69 and 2.04 in a ratio of 1:1, as a result of the two alternative deuterium environments. The presence of the C(H)D group in **13a** and **13b** clearly implicates the =C=C(H)D vinylidene intermediate in the reaction.

When it is heated to reflux temperatures in THF, compound **13** reacts with $CNBu^t$ to give $[Ru(CO)(PPh_3)(CNBu^t)(\eta^5\text{-}9\text{-}C(H){=}CH_2\text{-}7,8\text{-}C_2B_9H_{10})]$ (**14**), data for which are given in Tables 1−3. However, to establish the structure unambiguousy, an X-ray crystallographic study was carried out. Selected structural parameters are listed in Table 6, and the molecule is shown in Figure 4. The ruthenium is coordinated on one side by the CO, PPh_3, and $CNBu^t$ groups and on the other by the *nido*-$9\text{-}C(H){=}CH_2\text{-}7,8\text{-}C_2B_9H_{10}$ framework. Hence, **14** is derived from **13** by displacement of the $\eta^2\text{-}C(H){=}CH_2$ moiety in the latter by the $CNBu^t$ molecule in a process similar to the formation of **11** from **9**. The reaction of **13** with PMe_3 follows a different pathway, yielding the ylide complex $[Ru(CO)(PPh_3)\{\sigma{:}\,\eta^5\text{-}9\text{-}C(H)(PMe_3)CH_2\text{-}7,8\text{-}C_2B_9H_9\}]$ (**15**) (Tables 1−3). The NMR data are in agreement with the formulation. The ^1H and $^{13}C\{^1H\}$ NMR spectra show resonances for the cage CH groups at δ 0.40 and 2.39 and at δ 30.4 and 47.2, respectively. Peaks for the $BC(H)P{-}CH_2$ group occur in the ^1H spectrum at δ 1.18, 1.53, and 2.18 with the expected ^1H and ^{31}P couplings and in the $^{13}C\{^1H\}$ spectrum at δ 22.7 and 18.1 (Table 2), reflecting the saturated nature of the carbon atoms. The former signal is broad, as expected due to the nearby boron ^{11}B nuclei. In the $^{31}P\{^1H\}$ NMR spectrum the PMe_3 and PPh_3 groups give rise to two resonances at δ 24.2 and 50.9, respectively, as expected. The ylide complex $[Ru(CO)_2\{\sigma{:}\eta^5\text{-}10\text{-}C(H)(PMe_2Ph)CH_2\text{-}7,8\text{-}C_2B_9H_{10}\}]$, related to **15**, was obtained earlier as the product of the reaction of PMe_2Ph with $[Ru(CO)_2\{\eta^2{:}\eta^5\text{-}10\text{-}C(H){=}CH_2\text{-}7,8\text{-}C_2B_9H_{10}\}]$.[2b]

Scheme 1. Formation of the Deuterated Complexes 13a and 13b[a]

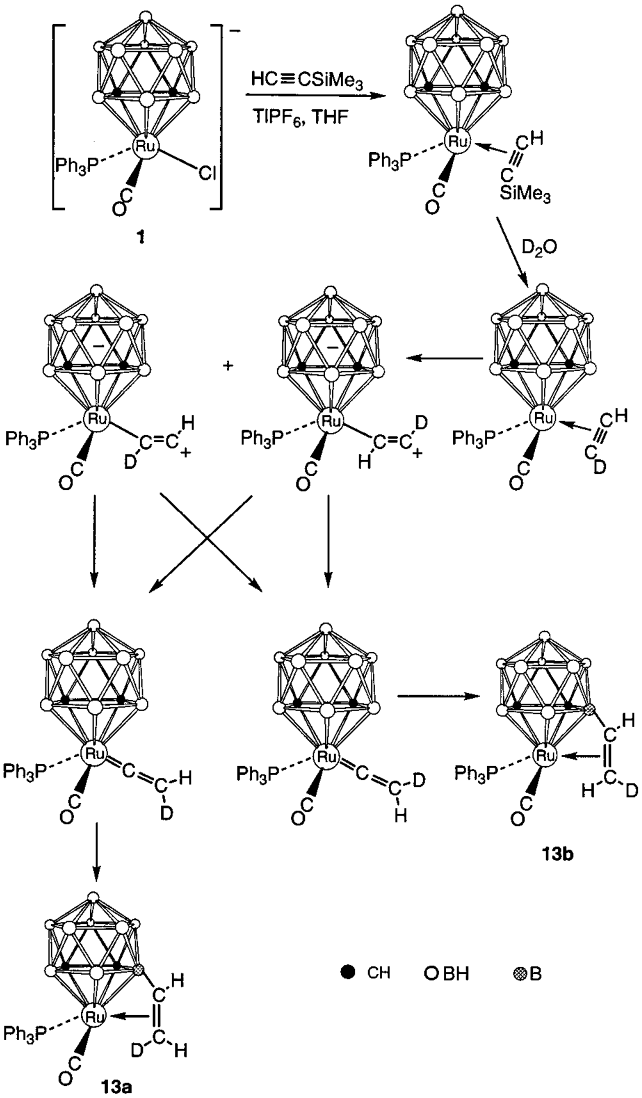

[a] The basic mechanism is taken from ref 8.

Conclusions

The results described in this paper together with those reported earlier[2b] show that the two fragments $Ru(CO)(L)(\eta^5\text{-}7,8\text{-}C_2B_9H_{11})$ (L = CO, PPh_3) display different reactivity patterns toward alkenes and alkynes. Several stable compounds of the formulation $[Ru(CO)_2(alkene)(\eta^5\text{-}7,8\text{-}C_2B_9H_{11})]$ exist, as do alkyne complexes of the type $[Ru(CO)_2(RC{\equiv}CR')(\eta^5\text{-}7,8\text{-}C_2B_9H_{11})]$, while the presence of the phosphine PPh_3 in place of a CO prevents stable alkene or internal alkyne coordination. Whereas in reactions with monosubstituted alkynes $RC{\equiv}CH$ compounds with up to three cage $B{-}(E)\text{-}C(H){=}C(H)R$ groups can be isolated from reactions involving the $Ru(CO)_2(\eta^5\text{-}7,8\text{-}C_2B_9H_{11})$ fragment, only species with

---

(8) Silvestre, J.; Hoffmann, R. *Helv. Chim. Acta* **1985**, *68*, 1461.

(9) (a) Bruce, M. I.; Swincer, A. G. *Adv. Organomet. Chem.* **1983**, *22*, 59. (b) Bruce, M. I. *Chem. Rev.* **1991**, *91*, 197.

Table 6. Selected Internuclear Distances (Å) and Angles (deg) for $[Ru(CNBu^t)(CO)(PPh_3)\{\eta^5\text{-}9\text{-}C(H){=}CH_2\text{-}7,8\text{-}C_2B_9H_{10}\}]\cdot CH_2Cl_2$ (14)

Ru−C(3)	1.846(4)	Ru−C(6)	1.989(4)	Ru−B(5)	2.251(4)	Ru−C(1)	2.256(3)
Ru−C(2)	2.262(3)	Ru−B(4)	2.287(4)	Ru−B(3)	2.305(4)	Ru−P	2.3366(9)
B(3)−C(4)	1.571(7)	C(3)−O(3)	1.145(4)	C(4)−C(5)	1.347(13)	C(6)−N(6)	1.152(4)
N(6)−C(7)	1.453(4)						
C(3)−Ru−C(6)	92.1(2)	C(5)−C(4)−B(3)	124.2(8)	B(4)−Ru−P	119.75(11)	C(6)−Ru−B(4)	151.6(2)
C(3)−Ru−C(1)	159.15(14)	N(6)−C(7)−C(9)	107.2(3)	C(4)−B(3)−B(8)	122.7(4)	C(3)−Ru−P	88.78(11)
C(6)−Ru−C(2)	87.65(14)	N(6)−C(7)−C(8)	107.8(3)	C(4)−B(3)−Ru	111.2(3)	C(1)−Ru−P	101.22(10)
C(3)−Ru−B(3)	90.9(2)	C(3)−Ru−B(5)	117.8(2)	N(6)−C(6)−Ru	175.2(3)	B(3)−Ru−P	166.57(11)
C(6)−Ru−P	88.04(10)	C(6)−Ru−C(1)	106.40(14)	N(6)−C(7)−C(10)	107.1(3)	C(4)−B(3)−B(7)	115.1(3)
C(2)−Ru−P	138.74(11)	C(3)−Ru−B(4)	83.2(2)	C(9)−C(7)−C(8)	112.0(4)	O(3)−C(3)−Ru	175.4(3)
C(4)−B(3)−C(2)	121.6(4)	C(6)−Ru−B(3)	105.4(2)	C(6)−Ru−B(5)	149.9(2)	C(6)−N(6)−C(7)	178.0(4)
C(4)−B(3)−B(4)	130.0(4)	B(5)−Ru−P	88.99(11)	C(3)−Ru−C(2)	132.4(2)	C(9)−C(7)−C(10)	111.5(4)

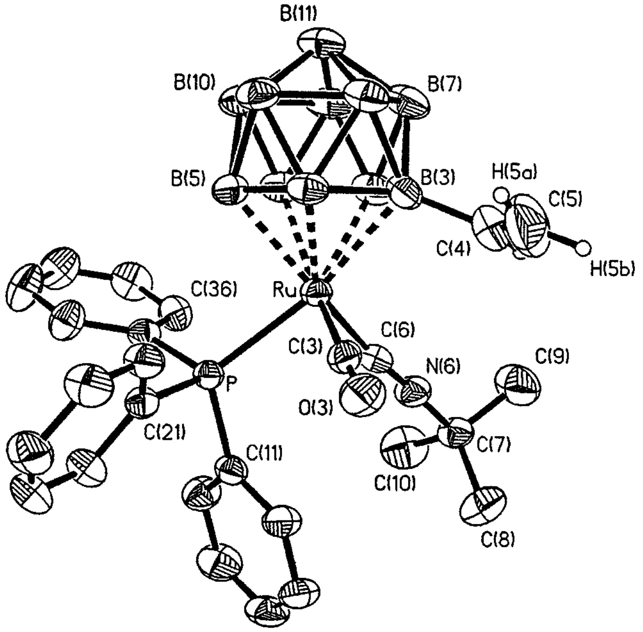

Figure 4. Structure of $[Ru(CNBu^t)(CO)(PPh_3)\{\eta^5\text{-}9\text{-}C(H){=}CH_2\text{-}7,8\text{-}C_2B_9H_{10}\}]$ (**14**), showing the crystallographic labeling scheme. Except for H(4a), H(5a), and H(5b), hydrogen atoms are omitted for clarity, and thermal ellipsoids are shown at the 40% probability level.

up to two such groups are formed when the $Ru(CO)(PPh_3)(\eta^5\text{-}7,8\text{-}C_2B_9H_{11})$ fragment is the precursor. Another difference in the behavior of the two fragments toward the alkynes RC≡CH is that the phosphine-containing precursor directs cage substitution to an α-boron site in the $\overline{\mathrm{CC}B\mathrm{BB}}$ ring ligating the ruthenium, whereas mixtures of α- and β-isomers are formed in reactions involving $Ru(CO)_2(\eta^5\text{-}7,8\text{-}C_2B_9H_{11})$. The synthesis of **13** from $Me_3SiC{\equiv}CH$ adds to the growing number of known reactions where the silyl group is cleaved following coordination of the alkyne to the metal.

Experimental Section

General Considerations. All experiments were conducted under an atmosphere of dry nitrogen using Schlenk tube techniques. Solvents were freshly distilled under nitrogen from appropriate drying agents before use. Light petroleum refers to that petroleum ether fraction of boiling point 40−60 °C. Chromatography columns (ca. 20 cm in length and 2 cm in diameter, unless otherwise stated) were packed with silica gel (Acros, 60−200 mesh). TLC was performed on preparative UNIPLATES (silica gel G, Analtech). Celite pads, used where necessary for filtration, were ca. 3 cm in length and 2 cm in diameter. The NMR measurements were recorded at the following frequencies: ^1H at 360.13 MHz, ^{13}C at 90.56 MHz, ^{11}B at 115.55 MHz, and ^{31}P at 145.78 MHz. The $^1H-^1H$ COSY45 NMR spectrum of **9** in CD_2Cl_2 required a 512 × 1024 point spectral matrix, with 8 transients per 1024 time-domain points, giving an accumulation time of ca. 9 min in total. For the transformation, sine-bell window functions were used for both the f1 and f2 dimensions. The reagents $[K(18\text{-crown-}6)][RuH(L)(PPh_3)(\eta^5\text{-}7,8\text{-}C_2B_9H_{11})]$ (L = CO, PPh_3) and $[Ru(CO)(PPh_3)_2(\eta^5\text{-}7,8\text{-}C_2B_9H_{11})]$ were prepared as described previously.[1]

Synthesis of $[K(18\text{-crown-}6)][RuCl(CO)(PPh_3)(\eta^5\text{-}7,8\text{-}C_2B_9H_{11})]$. An Et_2O (ca. 10 mL) suspension of $[K(18\text{-crown-}6)][RuH(CO)(PPh_3)(\eta^5\text{-}7,8\text{-}C_2B_9H_{11})]$ (0.05 g, 0.06 mmol) was treated with an excess of $HCl\cdot Et_2O$ and the mixture stirred overnight, affording a red-orange solid. After removal of solvent in vacuo the residue was crystallized twice from $CH_2Cl_2-Et_2O$ to afford analytically pure deep orange or red crystals of $[K(18\text{-crown-}6)][RuCl(CO)(PPh_3)(\eta^5\text{-}7,8\text{-}C_2B_9H_{11})]$ (**1**; 0.05 g).

Synthesis of $[K(18\text{-crown-}6)][RuCl(PPh_3)_2(\eta^5\text{-}7,8\text{-}C_2B_9H_{11})]$. A rapidly stirred Et_2O (ca. 10 mL) suspension of $[K(18\text{-crown-}6)][RuH(PPh_3)_2(\eta^5\text{-}7,8\text{-}C_2B_9H_{11})]$ (0.05 g, 0.05 mmol), cooled to ca. −78 °C, was treated dropwise with 1 mol equiv of $HCl\cdot Et_2O$ and the mixture stirred for 1−2 h, giving a red-orange solid. Overly rapid addition of HCl or insufficient cooling results in the formation of significant amounts of $[Ru(H)_2(PPh_3)_2(\eta^5\text{-}7,8\text{-}C_2B_9H_{11})]$. After removal of solvent in vacuo, crystallization and recrystallization of the solid from $CH_2Cl_2-Et_2O$ afforded analytically pure deep red crystals of $[K(18\text{-crown-}6)][RuCl(PPh_3)_2(\eta^5\text{-}7,8\text{-}C_2B_9H_{11})]$ (**2**; 0.04 g).

Synthesis of $[NEt_4][RuI(CO)(PPh_3)(\eta^5\text{-}7,8\text{-}C_2B_9H_{11})]$. The compounds $[Ru(CO)(PPh_3)_2(\eta^5\text{-}7,8\text{-}C_2B_9H_{11})]$ (0.50 g, 0.60 mmol) and NEt_4I (0.16 g, 0.60 mmol) were placed in a Schlenk tube, which was evacuated. After addition of THF (30 mL) the resulting suspension was brought gradually to a brisk reflux. Heating was continued for 1−2 days, affording a red solution. Completion of the reaction was determined by disappearance of the IR band at 1963 cm^{-1} due to $[Ru(CO)(PPh_3)_2(\eta^5\text{-}7,8\text{-}C_2B_9H_{11})]$ and the growth of the band at 1940 cm^{-1} due to the product. Solvent was removed in vacuo, the residue taken up in CH_2Cl_2 (10 mL), and the mixture cooled to 0 °C overnight. After removal of a white precipitate by filtration through Celite, solvent was evaporated to give a deep red oil, which was washed with benzene (3 × 10 mL), dissolved in the minimum of CH_2Cl_2 (ca. 5 mL), and layered with Et_2O. After interdiffusion of the two solvents deep red crystals formed, which were washed successively with EtOH (10 mL) and Et_2O (10 mL) and dried in vacuo to afford $[NEt_4][RuI(CO)(PPh_3)(\eta^5\text{-}7,8\text{-}C_2B_9H_{11})]$ (**3**; 0.48 g).

Synthesis of $[Ru(CNBu^t)(CO)(PPh_3)(\eta^5\text{-}7,8\text{-}C_2B_9H_{11})]$. A mixture of $[Ru(CO)(PPh_3)_2(\eta^5\text{-}7,8\text{-}C_2B_9H_{11})]$ (0.05 g, 0.06 mmol) and $CNBu^t$ (0.01 mL, 0.06 mmol) in CH_2Cl_2 (30 mL) was refluxed for ca. 12 h, affording a pale yellow solution. Solvent was removed in vacuo and the residue triturated with Et_2O (10 mL) to afford a crude off-white solid. The residue was

Table 7. Data for X-ray Crystal Structure Analyses

	3	**8**	**14**
cryst dimens (mm)	0.40 × 0.30 × 0.30	0.71 × 0.17 × 0.13	0.74 × 0.32 × 0.22
formula	$C_{29}H_{46}B_9INOPRu\cdot 0.5CH_2Cl_2$	$C_{29}H_{32}B_9OPRu$	$C_{28}H_{37}B_9NOPRu\cdot CH_2Cl_2$
M_r	823.36	625.88	717.84
cryst color, shape	red-orange blocks	orange needles	yellow needles
cryst syst	monoclinic	triclinic	monoclinic
space group	$P2_1/c$	$P\bar{1}$	$P2_1/n$
a (Å)	10.1874(23)	9.477(2)	10.5524(14)
b (Å)	29.2144(16)	10.7559(12)	21.874(3)
c (Å)	13.2192(12)	16.343(2)	16.1080(11)
α (deg)		109.085(10)	
β (deg)	104.392(11)	94.810(13)	102.821(8)
γ (deg)		107.214(12)	
V (Å$^{3)}$	3810.8(10)	1481.6(3)	3625.4(7)
Z	4	2	4
d_{calcd} (g cm^{-3})	1.435	1.403	1.316
μ(Mo Kα) (cm^{-1})	13.6	6.07	6.48
F(000) (e)	1652	636	1464
T (K)	293	293	293
2θ range (deg)	3.5−50.0	4.0−45.0	3.2−50.0
no. of rflns coll (excld stds)	6944	4131	6715
no. of unique rflns	6554	3852	6361
no. of obsd rflns	5114	3432	5070
rfln limits: h, k, l	−12 to 0, 0 to +34, −15 to +15	−10 to 0, −11 to +11, −17 to +17	0 to +12, 0 to +25, −19 to +18
no. of params refined	452	376	438
final residuals wR2 (R1), all data	0.0891 (0.0388)[a]	0.0799 (0.0300)[a]	0.0890 (0.0353)[a]
weighting factors[a]	$a = 0.0278$, $b = 7.4759$	$a = 0.0447$, $b = 0.8938$	$a = 0.0208$, $b = 4.5979$
goodness of fit on F^2	1.068	1.092	1.090
final electron density diff features (max/min) (e Å^{-3})	0.513, −0.434	0.351, −0.444	0.421, −0.663

[a] Refinement was block full-matrix least squares on all F^2 data: $wR2 = [\sum\{w(F_o^2 - F_c^2)^2\}/\sum w(F_o^2)^2]^{1/2}$, where $w^{-1} = [\sigma^2(F_o^2) + (aP)^2 + bP]$ and $P = [\max(F_o^2,0) + 2F_c^2]/3$. The value in parentheses is given for comparison with refinements based on F_o with a typical threshold of $F_o > 4\sigma(F_o)$ and $R1 = \sum||F_o| - |F_c||/\sum|F_o|$ and $w^{-1} = [\sigma^2(F_o) + g(F_o^2)]$.

dissolved in CH_2Cl_2 (2 mL), whereupon diffusion into an Et_2O layer at 25 °C gave a colorless powder which was washed successively with ethanol (2 × 10 mL) and petroleum ether (10 mL) and dried in vacuo to give [Ru(CNBu^t)(CO)(PPh$_3$)(η^5-7,8-$C_2B_9H_{11}$)] (**4**; 0.04 g).

Reactions of [K(18-crown-6)][RuCl(CO)(PPh$_3$)(η^5-7,8-$C_2B_9H_{11}$)] with Alkynes. (i) Compound **1** (0.10 g, 0.12 mmol) and $TlPF_6$ (0.04 g, 0.12 mmol) were placed in a Schlenk tube, which was evacuated, and THF (20 mL) was added. The mixture was stirred for 1 h, and the resultant orange suspension was treated with PhC≡CH (0.04 mL, 0.36 mmol) and further stirred for 20 min. Separation by TLC using CH_2Cl_2−petroleum ether (1:3) as eluant gave a major yellow band (R_f = 0.62) from which [Ru(CO)(PPh$_3$)(η^2: η^5-9-(E)-C(H)=C(H)Ph-7,8-$C_2B_9H_{10}$)] (**8**) was isolated (0.04 g).

(ii) Similarly **1** (0.10 g, 0.12 mmol) and $TlPF_6$ (0.04 g, 0.12 mmol) were stirred in THF (20 mL) for 1 h and Bu^{t}C≡CH (0.04 mL, 0.36 mmol) was added. The suspension was further stirred overnight. Solvent was removed in vacuo, the residue dissolved in the minimum of CH_2Cl_2 (ca. 5 mL), and the mixture chromatographed. Elution with CH_2Cl_2−petroleum ether (1:4) gave an orange fraction, which on removing the solvent in vacuo and washing the residue with petroleum ether yielded orange microcrystals of [Ru(CO)(PPh$_3$){η^2: η^5-9-(E)-C(H)=C(H)-Bu^t-10-C(H)=C(H)Bu^t-7,8-$C_2B_9H_9$}] (**9**; 0.05 g).

(iii) Compounds **1** (0.10 g, 0.12 mmol) and $TlPF_6$ (0.04 g, 0.12 mmol) were placed in a Schlenk tube, which had been evacuated, and THF (20 mL) was added. After it was stirred for 1 h, the orange suspension was treated with Me$_3$SiC≡CH (0.05 mL, 0.35 mmol), with stirring continued overnight. The mixture was then chromatographed, and elution with CH_2Cl_2−petroleum ether (1:3) removed a broad yellow band. Evaporating the solvent in vacuo from the eluate and washing the residue with petroleum ether gave yellow microcrystals of [Ru(CO)(PPh$_3$)(η^2: η^5-9-C(H)=CH$_2$-7,8-$C_2B_9H_{10}$)] (**13**; 0.06 g).

Synthesis of [Ru(CO)(PMe$_3$)(PPh$_3$)(η^5-9,10-{(E)-C(H)=C(H)Bu^t}$_2$-7,8-$C_2B_9H_9$)]. Compound **9** (0.05 g, 0.07 mmol), dissolved in petroleum ether (40 mL), was treated with PMe$_3$ (0.07 mL, 1 M in THF). Instantaneous formation of a yellow precipitate was observed. After the mixture was stirred for 3 h, the solvent was decanted and the residue was washed with petroleum ether (3 × 10 mL) to yield a yellow powder of [Ru(CO)(PMe$_3$)(PPh$_3$)(η^5-9,10-{(E)-C(H)=C(H)Bu^t}$_2$-7,8-$C_2B_9H_9$)] (**10**; 0.05 g).

Synthesis of [Ru(CNBu^t)(CO)(PPh$_3$)(η^5-9,10-{(E)-C(H)=C(H)Bu^t}$_2$-7,8-$C_2B_9H_9$)]. Compound **9** (0.05 g, 0.07 mmol), in THF (20 mL), was treated with CNBu^t (0.03 mL, 0.27 mmol). The color of the solution immediately changed from orange to yellow. After the mixture had been stirred for 1 h, the solvent was removed in vacuo and the residue dissolved in CH_2Cl_2 (ca. 2 mL) and chromatographed. Elution with CH_2Cl_2−petroleum ether (1:1) removed a yellow fraction, which after evaporating the solvent in vacuo and washing the oily residue with petroleum ether (2 × 5 mL) yielded [Ru(CNBu^t)(CO)(PPh$_3$)-(η^5-9,10-{(E)-C(H)=C(H)Bu^t}$_2$-7,8-$C_2B_9H_9$)] (**11**; 0.05 g) as a yellow solid.

Synthesis of [Ru(CO)$_2$(PPh$_3$)(η^5-9,10-{(E)-C(H)=C(H)-Bu^t}$_2$-7,8-$C_2B_9H_9$)]. Compound **9** (0.05 g, 0.07 mmol) was dissolved in THF (20 mL), and CO was bubbled through the solution for 3 h, during which time the color changed from orange to yellow. Solvent was removed in vacuo and the residue dissolved in CH_2Cl_2 (ca. 2 mL) and chromatographed. Elution with CH_2Cl_2−petroleum ether (2:3) removed a yellow fraction, which on evaporating the solvent and washing the oily residue with petroleum ether (2 × 5 mL) afforded [Ru(CO)$_2$(PPh$_3$)(η^5-9,10-{(E)-C(H)=C(H)Bu^t}$_2$-7,8-$C_2B_9H_9$)] (**12**; 0.04 g) as yellow microcrystals.

Synthesis of [Ru(CNBu^t)(CO)(PPh$_3$)(η^5-9-C(H)=CH$_2$-7,8-$C_2B_9H_{10}$)]. Compound **13** (0.05 g, 0.09 mmol) was dissolved in THF (20 mL) with CNBu^t (0.04 mL, 0.36 mmol) and the mixture heated to reflux overnight. After the mixture was cooled to room temperature, solvent was removed in vacuo and the residue dissolved in CH_2Cl_2 (2 mL) and chromatographed. Elution with CH_2Cl_2−petroleum ether (1:1) removed a yellow fraction, which on evaporation of solvent in vacuo yielded pale yellow microcrystals of [Ru(CNBu^t)(CO)(PPh$_3$)(η^5-9-C(H)=CH$_2$-7,8-C$_2$B$_9$H$_{10}$)] (**14**; 0.05 g).

Synthesis of [Ru(CO)(PPh$_3$)(σ:η^5-9-C(H)(PMe$_3$)CH$_2$-7,8-C$_2$B$_9$H$_{10}$)]. Compound **13** (0.05 g, 0.09 mmol) was dissolved in petroleum ether (30 mL), and PMe$_3$ (0.11 mL,1 M in THF) was added. The suspension was stirred for 3 h, and the solvent was decanted to give pale yellow microcrystals of [Ru(CO)(PPh$_3$)(σ: η^5-9-C(H)(PMe$_3$)CH$_2$-7,8-C$_2$B$_9$H$_9$)] (**15**; 0.05 g).

Crystal Structure Determinations and Refinements. Experimental data for **3**, **8**, and **14** are shown in Table 7. Those for **9** and **13** are provided in the Supporting Information. Diffracted intensities were collected on an Enraf-Nonius CAD-4 operating in the $\omega-2\theta$ scan mode, using graphite-monochromated Mo Kα X-radiation. Final unit cell dimensions were determined from the setting angles of 25 accurately centered reflections. Crystal stability during the data collection was monitored by measuring the intensities of three standard reflections every 2 h. Data were collected at a varied rate of 4.13−5.17° min^{-1} in ω with a scan range of $1.15 + 0.34 \tan \theta$ for **3**, a constant scan speed of 5.17° min^{-1} in ω with a scan range of $0.95 + 0.34 \tan \theta$ for **13**, a constant scan speed of 5.17° min^{-1} in ω with a scan range of $1.15 + 0.34 \tan \theta$ for **8** and **14**, and a varied rate of 4.13−5.17° min^{-1} in ω with a scan range of $1.00 + 0.34 \tan \theta$ for **9**. The data were corrected for Lorentz, polarization, and X-ray absorption effects, the last using either a face-indexed method based on the measurements of 6 crystal faces for **8**, **13**, and **14** or a semiempirical method based on azimuthal scans of ψ-data for **3** and **9**.

The structures were solved by direct methods, and successive difference Fourier syntheses were used to locate all non-hydrogen atoms using SHELXTL version 5.03.[10] Refinements were made by full-matrix least squares on all F^2 data using SHELXL-97.[11] Anisotropic thermal parameters were included for all non-hydrogen atoms. Cage carbon atoms were assigned by comparison of the bond lengths to adjacent boron atoms in conjunction with the magnitudes of their equivalent isotropic thermal parameters. All hydrogen atoms, except the transoid hydrogens of the various pendant groups, were included in calculated positions and allowed to ride on their parent boron or carbon atoms with fixed isotropic thermal parameters ($U_{iso} = 1.2U_{iso}$ of the parent atom except for Me protons, where $U_{iso} = 1.5U_{iso}$). Hydrogens H(4a) and H(5a) for **8**, H(4a), H(5a), H(10a), and H(11a) for **9**, H(4a), H(5a), and H(5b) for **13**, and H(5a), H(5b), H(5a1), and H(5b1) for **14** were located in difference Fourier maps, and their positional parameters were refined while their isotropic thermal parameters were constrained to 1.2 times the U_{iso} value of the parent carbon atoms.

The ethyl groups of the [NEt$_4$] cation in **3** were disordered, with each methylene carbon atom (C(51), C(53), C(55), and C(57); C(51A), C(53A), C(55A), and C(57A)) occupying two distinct sites. The methyl carbon atoms (C(52), C(54), C(56), and C(58); C(52A), C(54A), C(56A), and C(58A)) were constrained with the same positional and thermal parameters. The site occupancy factors were fixed at 0.5. Compound **3** also crystallized with a molecule of CH$_2$Cl$_2$, which was found to reside near a center of inversion and was refined with a site occupancy factor of 0.5. This molecule was disordered, as is evident from the high thermal parameters and the residual electron density in the difference Fourier syntheses located in this region, but no attempt was made to resolve the disorder. The bond lengths and angles of the CH$_2$Cl$_2$ group were restrained. The methyl groups of one of the CH=CHBu^t ligands in **9** are disordered over two sites such that the two sets of methyl substituents are rotated 30° about the C(11)−C(12) bond. The pendant CH=CH$_2$ group in **14** was disordered over two sites in a 60:40 ratio. The chlorine atoms of the solvent molecule of **14** are disordered over two sites (70:30). In **3**, residual electron density was located in the vicinity of the disordered CH$_2$Cl$_2$ molecule. In **8**, **9**, **13**, and **14** insignificant residual electron density in the difference Fourier syntheses was found near the Ru atoms.

Acknowledgment. We thank the Robert A. Welch foundation for support (Grant AA-1201).

Supporting Information Available: Tables of atomic coordinates and U values, bond lengths and angles, and anisotropic thermal parameters for **3**, **8**, **9**, **13**, and **14** in CIF format and a ^{2}H NMR spectrum of the mixture of complexes **13a** and **13b**. This material is available free of charge via the Internet at http://pubs.acs.org.

OM000018I

---

(10) SHELXTL version 5.03; Bruker AXS, Madison, WI, 1995.

(11) Sheldrick, G. M. University of Göttingen, Göttingen, Germany, 1997.